

1 **Title:** Transcriptome and epigenome analyses of vernalization in *Arabidopsis thaliana*

2

3 **Authors:** Yanpeng Xi <sup>1</sup>, Sung-Rye Park <sup>1</sup>, Dong-Hwan Kim <sup>1</sup>, Eun-Deok Kim <sup>1</sup>, and Sibusung

4 <sup>1,2</sup>

5

6 **Affiliations:** <sup>1</sup> Department of Molecular Biosciences, The University of Texas at Austin, Austin,

7 TX, 78712, USA, <sup>2</sup> International Scholar, Kyung-Hee University, Suwon, Korea

8

9 Yanpeng Xi: [yanpengxi@utexas.edu](mailto:yanpengxi@utexas.edu)

10 Sung-Rye Park: [pasungry@umich.edu](mailto:pasungry@umich.edu)

11 Eun-Deok Kim: [eundeok@uw.edu](mailto:eundeok@uw.edu)

12 Dong-Hwan Kim: [dhkim92@cau.ac.kr](mailto:dhkim92@cau.ac.kr)

13 Sibusung Sung: [sbsung@austin.utexas.edu](mailto:sbsung@austin.utexas.edu)

14

15

16 Correspondence should be addressed to: Sibusung Sung, [sbsung@austin.utexas.edu](mailto:sbsung@austin.utexas.edu)

17 **Abstract**

18 **Background:** Vernalization accelerates flowering after prolonged winter cold. Transcriptional and  
19 epigenetic changes are known to be involved in the regulation of the vernalization response.  
20 Despite intensive applications of next-generation sequencing in diverse aspects of plant research,  
21 genome-wide transcriptome and epigenome profiling during vernalization response has not been  
22 conducted.

23  
24 **Results:** In this work, we present the first comprehensive analyses of transcriptomic and  
25 epigenomic dynamics during the vernalization process in *Arabidopsis thaliana*. Six major clusters  
26 of genes exhibiting distinctive features were identified. Temporary changes in histone H3K4me3  
27 levels were observed that likely coordinate photosynthesis and prevent oxidative damage during  
28 cold. In addition, vernalization induced a stable accumulation of H3K27me3 over genes encoding  
29 many development-related transcription factors, resulting in either inhibition of transcription or a  
30 bivalent status of the genes. Lastly, *FLC*-like and *VIN3*-like genes were identified that appear to  
31 be novel components of the vernalization pathway.

32  
33 **Conclusions:** Our work provides the first comprehensive assessment of transcriptome and  
34 epigenome dynamics during the vernalization process and indicates that multiple regulatory  
35 pathways are involved in promoting differentiation and phase transitions during vernalization in  
36 *Arabidopsis*.

37  
38 **Keywords:** Vernalization, Transcriptome, Histone modification, RNA-seq, ChIP-seq,  
39 *Arabidopsis*

## 40 **Background**

41       Temperature is an important environmental cue that, coupled with day length, cues plants to  
42 initiate flowering. For most winter-annual and biennial plants, prevention of flowering before  
43 winter and induction of flowering after winter is required for successful reproduction. Cold itself  
44 is not sufficient since temperature fluctuations in fall might be falsely taken as the passing of winter.  
45 A timing mechanism is needed to distinguish long-term winter cold from short-term chilling stress.  
46 Therefore, the vernalization process evolved which accelerates flowering only after prolonged cold  
47 exposure. In winter-annual *Arabidopsis thaliana*, vernalization is regulated by two major loci:  
48 *FLOWERING LOCUS C (FLC)* and *FRIGIDA (FRI)* [1-3]. *FLC* encodes a MADS-box  
49 transcription factor that represses the expression of downstream targets [4-6]. *FRI* acts with other  
50 proteins in a complex to upregulate *FLC* expression [7-14]. High level of *FLC* and its clade  
51 members prevent flowering by repressing floral integrator genes such as *FLOWERING LOCUS T*  
52 (*FT*) and *SUPPRESSOR OF OVEREXPRESSION OF CONSTANS 1 (SOC1)* [6, 15-20] and also  
53 feedback regulations operate between *FLC* and floral integrators [21, 22], forming intricate  
54 regulatory networks that control flowering. *FLC* is stably repressed by prolonged winter cold,  
55 thereby enables rapid induction of flowering under favorable day length in spring. The  
56 vernalization-triggered *FLC* repression is mitotically stable and it is reset only during meiosis to  
57 ensure the requirement of vernalization in the next generation [23]. This “memory” of winter  
58 indicates the involvement of epigenetic regulation. Indeed, studies performed during the past  
59 decade have begun to elucidate the role of histone modification and chromatin structural dynamics  
60 in *FLC* repression [24-34].

61       Before vernalization, *FLC* chromatin is enriched with active histone marks, including histone  
62 acetylation, H3K4me3, H3K36me3, and etc., which are likely deposited by *FRI* complexes [8, 12,

63 35-37]. Early in vernalization, the expression of antisense noncoding RNAs are induced at *FLC*  
64 locus. Expression of these RNAs, termed *COOLAIR* (cold induced long antisense intragenic RNA)  
65 correlates with the reduction in expression of the *FLC* sense transcript, and *COOLAIR* physically  
66 associates with *FLC* chromatin resulting in depletion of H3K36me3 [38, 39]. Recently, expression  
67 of *VPI/ABI3-LIKE1 (VAL1)* was shown to be necessary for vernalization-mediated reduction of  
68 histone acetylation at *FLC*. VAL1 is a B3 domain protein recruited to *FLC* through its direct  
69 binding to RY motifs within the nucleation region. VAL1 recruits histone deacetylase HDA19 to  
70 *FLC* chromatin [33, 40].

71 In late stage of vernalization, prolonged cold induces sufficient amount of  
72 VERNALIZATION INSENSITIVE 3 (VIN3), a PHD-finger domain protein, which forms  
73 heterodimer with VIN3-LIKE 1 (VIL1) and together recruit POLYCOMB REPRESSIVE  
74 COMPLEX 2 (PRC2) to the nucleation region in the first intron of *FLC*. This PHD-PRC2 complex  
75 catalyzes the tri-methylation of histone H3K27, a well-characterized repressive mark [28]. At this  
76 stage, H3K27me3 modifications are confined within the nucleation region. Meanwhile, expression  
77 of another noncoding RNA, termed *COLD AIR* (cold assisted intronic noncoding RNA) is induced  
78 from the sense direction of the first intron of *FLC*. Loss of *COLD AIR* results in a vernalization-  
79 insensitive phenotype [30]. *COLD AIR* interacts with CURLY LEAF (CLF), the enzymatic core of  
80 PRC2, to facilitate its sequence-specific binding at the *FLC* locus [30, 34]. When temperatures  
81 warm, VIN3 levels decline rapidly, but VIL1-PRC2 remains bound to the *FLC* locus. H3K27me3  
82 spreads until it covers the entire genomic region of *FLC*. It is not clear how or why the spreading  
83 of repressive marks occurs only when the temperature warms. The accelerated enzymatic activity  
84 of histone modifying complexes at higher temperatures might explain this phenomenon. LIKE  
85 HETEROCHROMATIN PROTEIN 1 (LHP1) proteins are enriched at *FLC* following PRC2

86 action, and these proteins are necessary for stable maintenance of the epigenetically repressed state  
87 of *FLC* in warm conditions. *VAL1* recruits *LHP1* to *FLC* through direct protein-protein  
88 interactions [40]. The repressive state of *FLC* is stably inherited through many cycles of cell  
89 division during subsequent growth and development.

90 In addition to changes in histone modifications, chromatin structural changes also occur at  
91 *FLC* locus during vernalization. Vernalization induces physical clustering of *FLC* alleles in the  
92 nucleus, which requires Polycomb complex components *VERNALIZATION INSENSITIVE 2*  
93 (*VRN2*) and *VIL1*, but not *LHP1* [31]. An interaction between the 5' and 3' regions of the *FLC*  
94 chromatin is formed before cold and is disrupted during the early stage of vernalization. The  
95 mechanism of formation this loop is not clear. It is known that the transcriptional status of *FLC* is  
96 not relevant to this process and that the components of *PRC2* complex are not necessary [32]. An  
97 intragenic chromatin loop is also induced by vernalization, which could be responsible for the  
98 vernalization-induced spreading of *H3K27me3* marks along *FLC* chromatin [34]. A non-coding  
99 RNA derived from the *FLC* promoter called *COLDWRAP* is involved in the formation of the  
100 intragenic chromatin loop.

101 Given the quantitative nature of vernalization response, it would be helpful to have a  
102 comprehensive picture of the transcriptome and epigenome changes that occur during the  
103 vernalization process. To date, few vernalization-related next-generation sequencing datasets have  
104 been generated, and most come from food crops such as pak choi (*Brassica rapa subsp. chinensis*)  
105 and radish (*Raphanus sativus L.*) [41, 42]. The RNA-seq and ChIP-seq analyses collected at  
106 multiple time points during vernalization described in this work represent the first comprehensive  
107 profiling of the transcriptome and epigenome dynamics of vernalization in *Arabidopsis thaliana*.

108

## 109 **Results & Discussions**

### 110 **Transcriptional dynamics of vernalization in *Arabidopsis thaliana***

111 To capture genome-wide transcriptional dynamics during the vernalization process, seven  
112 samples were collected, termed NV (without cold exposure), V1h (1-hour cold), V1d (1-day cold),  
113 V10d (10-day cold), V20d (20-day cold), V40d (40-day cold), and T10 (40-day cold followed by  
114 10-day normal growth temperature). The well-known patterns of *FLC* repression and *VIN3*  
115 induction were successfully captured by the RNA-seq (Fig. 1A, 1B and Table S1). *FLC* belongs  
116 to a small gene family, including *FLC* and the *MADS AFFECTING FLOWERING* genes *MAF1*  
117 (also known as *FLOWERING LOCUS M*), *MAF2*, *MAF3*, *MAF4*, and *MAF5*. The RNA-seq data  
118 showed relatively similar dynamics of *MAF1* and *FLC* that differed from the patterns of expression  
119 of *MAF2* and *MAF3* (Fig. 1A). *MAF4* and *MAF5* were of too low abundance for a pattern of  
120 expression to be confidently differentiated by RNA-seq. Of the *VIN* family members, *VIL2* showed  
121 the highest expression, whereas *VIL3* was barely detected. Levels of *VIL1* and *VIL2* were largely  
122 stable across vernalization (Fig. 1B).

123 Differentially expressed genes (DEGs) were by comparison of vernalized samples to NV  
124 samples. All the time points, except V1h, showed similar numbers of up- and down-regulated  
125 genes (Fig. 1C). Only 710 up-regulated and 306 down-regulated genes were identified in V1h  
126 samples, indicating that the downstream cascades of cold-regulated genes were initiated by a  
127 limited number of early responsive genes. V10d, V20d, and V40d shared 3,485 differentially  
128 regulated genes in common (Fig. 1D), suggesting that expression of many cold-regulated genes  
129 was stably maintained regardless of the duration of cold. That 3,976 of the 5,580 genes expressed  
130 during V1d were also expressed at one or more of the V10d, V20d, and V40d time points indicate  
131 that long-term responses built up within just one day of cold exposure are maintained (Fig. 1E).

132

133 To fully explore the time-course dynamics, differentially expressed genes from all time  
134 points were clustered based on expression patterns. Six major clusters with distinct transcriptional  
135 dynamics were identified (Fig. 2). Cluster 1 consisted of a small number of early responsive genes  
136 (545) that were up- or down-regulation within just 1 hour of cold treatment (Fig. 2A). Gene  
137 Ontology (GO) analysis revealed that this cluster was enriched in hormone-related genes,  
138 including ethylene, abscisic acid, cytokinin, and salicylic acid (Fig. 2A), which is consistent with  
139 the fact that plant hormones are usually among the “first responders” upon environmental changes  
140 and stresses. Members of cluster 2 (2,272 genes) and cluster 3 (1,744 genes) exhibited relatively  
141 constant up- and down-regulation, respectively, at time points V1d to V40d (Fig. 2B, 2C),  
142 indicating that these genes are regulated during cold. GO analysis showed that up-regulated genes  
143 in cluster 2 were enriched in translation-related terms (Figure 2B), such as ribosome biogenesis,  
144 translation initiation, RNA secondary structure unwinding, and rRNA processing, suggesting that  
145 protein synthesis is boosted during prolonged cold, probably in order to make up for the reduced  
146 enzymatic activity at low temperature.

147 Photosynthesis and lipid processing genes were enriched in cluster 3 (Figure 2C),  
148 indicating that in *Arabidopsis* photosynthesis is repressed during cold. In evergreen plants, winter  
149 cold inhibits the efficiency of photosynthetic CO<sub>2</sub> assimilation, which could lead to over-excitation  
150 and increased photo-oxidative damage if plants continue to absorb light energy. Therefore, down-  
151 regulation of light absorption balances the supply and utilization of energy during cold and protect  
152 plants from photo-oxidative damage [43]. Indeed, the photosynthesis-related genes in cluster 3  
153 mostly encode components of light harvesting complexes, suggesting that *Arabidopsis* utilizes a  
154 similar strategy as evergreens during winter cold.

155 Genes in cluster 4 (911 genes) had expression that was gradually induced during cold  
156 instead as opposed to the constant high levels observed for genes in cluster 2 (Figure 2D). This  
157 pattern resembles that of *VIN3* during vernalization. Genes related to microtubule movement were  
158 present in this cluster. Genes in cluster 5 (1,828 genes) and cluster 6 (1,650 genes) had gradually  
159 increased or decreased expression during cold, respectively, and levels of these genes were  
160 maintained after the return to warm temperature (Figure 2E, 2F). The pattern of expression of  
161 genes in cluster 6 resembled that of *FLC* during vernalization. No functional terms showed obvious  
162 enrichment in these two clusters.

163 To identify potential protein binding motifs enriched in the six major clusters, 3 kilobases  
164 of promoter sequence for each gene were extracted and analyzed using the MEME program for  
165 motif discovery and analysis. Five major motifs were discovered with distinct and overlapping  
166 enrichment among the clusters (Fig. 2, far right; Table 1). Motif 1 (M1) was enriched in clusters  
167 3, 4, and 6 and motif 2 (M2) in clusters 2 and 5. Motif 3 (M3) and motif 4 (M4) were both enriched  
168 in clusters 2 and 4, and motif 5 (M5) was only enriched in cluster 2. Overall, gene clusters up-  
169 regulated during vernalization showed higher motif enrichment, suggesting that induction of genes  
170 was regulated by the combination of transcription factors, whereas repression might require  
171 distinct mechanisms. The transcription factors with binding motifs that match those enriched in  
172 genes differentially expressed during vernalization are listed in Table 2. Many of these  
173 transcription factors are involved in salt stress, hormone signaling, and flowering regulation. Motif  
174 4 was of great interest since it is the binding motif for the ERF/AP2 transcription factors involved  
175 in hypoxia signaling [44, 45], and *VIN3* was reported to be induced by hypoxia [46]. It is also  
176 noteworthy that a recent finding showed that hypoxia also stabilizes the VRN2-containing PRC2

177 complex to mediate the repression of *FLC* during vernalization [47], implicating biological  
178 relevance between hypoxia and vernalization.

179

### 180 **Histone modification changes during vernalization**

181 Three well-studied histone modifications, H3K27me3, H3K4me3, and H3K36me3, were  
182 analyzed by ChIP-seq at NV, V40d, and T10 (Fig. 3 and Table S2). We first analyzed the  
183 distribution of histone marks on *FLC* chromatin at these time points (Fig. 3A). An enrichment of  
184 H3K27me3 was observed around the *FLC* transcription start site at V40d compared to NV. The  
185 gene body of *FLC* exhibited a minor increase of H3K27me3 during cold, whereas the major  
186 spreading and coverage of repressive marks occurred only after plants were moved back to warm  
187 temperature at T10 (Fig. 3A). Consistent with the increase of H3K27me3, a decrease of  
188 H3K36me3 along the gene body of *FLC* was observed as a function of time, although the overall  
189 enrichment of H3K36me3 was much lower than that of H3K27me3 at all stages. To our surprise,  
190 the H3K4me3 marks showed little change during and after vernalization (Fig. 3A), which was  
191 quite different from previous reports showing that H3K4me3 undergone vernalization-induced  
192 reduction at *FLC* locus. Besides the transcription start site, a minor H3K4me3 peak was observed  
193 around the 3'-end of *FLC*. The function of this peak is unclear. We hypothesize that it could be  
194 involved in the formation of chromatin loop or the expression of antisense transcripts [38, 39].

195 At the genome-wide level, H3K4me3 and H3K36me3 were enriched on actively  
196 transcribed genes, whereas H3K27me3 was observed over genes expressed at low levels and over  
197 silenced genes (Fig. 3B). H3K4me3 peaks were confined around transcription start sites with an  
198 average span of about 2 kilobases, whereas H3K36me3 and H3K27me3 were diffused into gene  
199 bodies (Fig. 3C). Most of the H3K4me3 peaks did not change much in terms of location or intensity

200 during vernalization (Fig. 3D). H3K36me3 largely followed the pattern of H3K4me3 distribution  
201 (Fig. 3E, 3F) as expected since both are active histone marks. In total, 19,176, 18,804, and 19,176  
202 peaks were called for H3K4me3 in NV, V40d, and T10 samples, respectively, and 13,968, 13,859,  
203 and 13,601 peaks were called for H3K36me3 at these time points (Fig. 3D). These numbers  
204 represent two-thirds of coding genes in *Arabidopsis* genome, which roughly matches the number  
205 of actively transcribed genes. Thus, nearly every actively transcribed gene has an H3K4me3 peak  
206 located at their transcription start site. The lower numbers of genes marked by H3K36me3  
207 compared to H3K4me3 are probably due to the overall lower enrichment levels for H3K36me3  
208 compared to H3K4me3 detected in our ChIP-seq analysis. As expected due to the synergistic  
209 function of these modifications in transcriptional regulation, 98.6% of H3K36me3 peaks  
210 overlapped with an H3K4me3 peak (Fig. 3F).

211 A much smaller number of peaks were called for H3K27me3 than for the active histone  
212 marks, with 5,969, 7,463, and 7,236 peaks in NV, V40d, and T10 samples, respectively (Fig. 3D).  
213 Only 2.0% to 4.7% of peaks, depending on the time point, overlapped between these two marks.  
214 Surprisingly, a large portion of H3K27me3 peaks (33.2%) overlapped with H3K4me3 marks (Fig.  
215 3F), resulting in the so-called “bivalent” status for the underlying genes [48-51]. GO analysis  
216 indicated that transcription factors were highly enriched in the group of genes with bivalent histone  
217 marks, suggesting that the combination of H3K27me3 and H3K4me3 could be required for flexible  
218 regulation of transcription factors in *Arabidopsis*. The transcription factors with bivalent marks  
219 are listed in Supplemental Table S3.

220

221 **Vernalization causes an overall increase of H3K27me3 in *Arabidopsis* genome**

222 Vernalization had minimal effect on H3K36me3 distribution, as peaks from V40d and T10  
223 correlated almost perfectly with NV samples (Fig. 4A). A temporary effect of vernalization on  
224 H3K4me3 was enhanced diffusion at V40d; patterns of H3K4me3 at T10 were similar to those at  
225 NV. In contrast, vernalization-induced H3K27me3 changes observed at V40d were maintained  
226 after plants were moved back to warm temperature at T10 (Fig. 4A). To quantify the differential  
227 peaks among samples, reads within each peak were extracted and converted to digital counts for  
228 statistical analysis. Consistent with the correlation analysis, only 9.9% of H3K36me3 peaks were  
229 differentially regulated; a slightly higher percentage of H3K4me3 peaks (15.6%) were  
230 differentially regulated. In contrast, over one-third of H3K27me3 peaks (36.6%) were  
231 differentially regulated by vernalization (Fig. 4B). Surprisingly, the direction of change of these  
232 differentially regulated peaks was not evenly distributed: Cold induced an overall decrease of  
233 H3K4me3 and increase of H3K27me3 at V40d (Fig. 4C). The absence of down-regulated  
234 H3K27me3 peaks indicated a potential unidirectional action of H3K27me3 for switching off genes  
235 and suggests that, once added, the H3K27me3 mark is difficult to remove. To confirm the ChIP-  
236 seq results, several genes were randomly chosen for validation. Quantitative real-time PCR (qRT-  
237 PCR) showed validated the ChIP-seq analysis (Fig. S1).

238         The group of genes with cold-induced reduction of H3K4me3 were enriched with  
239 photosynthesis-related terms (Fig. 4D), as was cluster 3 of cold down-regulated genes (Fig. 2C).  
240 Therefore, it is likely that in *Arabidopsis* the temporary removal of H3K4me3 marks at the  
241 transcription start site decreases the expression of photosynthesis genes to prevent photo-oxidative  
242 damage during cold and quickly restores their activities in warm temperature to ensure normal  
243 growth and development. The factors involved in this temperature-induced H3K4me3 change are  
244 currently unknown.

245 Interestingly, transcription factors from almost all families were strongly enriched in the  
246 group of genes with H3K27me3 peaks up-regulated during vernalization (Fig. 4E). Of the 335  
247 transcription factor genes that had strongly up-regulated H3K27me3, 155 were marked also with  
248 H3K4me3 (Fig. 4F). GO analysis revealed that floral regulator genes were enriched in the group  
249 of transcription factors with vernalization-induced H3K27me3 modifications (Table 3),  
250 confirming that vernalization promotes the transition from vegetative growth to reproductive  
251 growth through epigenetic switching off of regulatory hub genes in *Arabidopsis*.

252

### 253 **Identification of *FLC*-like and *VIN3*-like transcripts**

254 We hypothesized that any gene with a repression pattern similar to that of *FLC* or an  
255 induction pattern similar to that of *VIN3* upon cold treatment could have similar functions during  
256 vernalization. Cluster 6 and cluster 4 included genes with patterns of expression similar to those  
257 of *FLC* and *VIN3*, respectively (Fig. 2D, 2F). A dynamic time warping (DTW) algorithm was used  
258 to identify optimal matches within each cluster. DTW was first used in speech recognition for  
259 measuring the similarity between soundtracks [52]. The advantage of DTW over simple pairwise  
260 comparison is that it allows the stretch and compression of input sequences. In this work, the time-  
261 series transcriptional dynamics of two genes were given as inputs, and a distance score was then  
262 calculated (Fig. 5A, 5B). The lower the distance score, the higher the similarity of the two  
263 expression patterns (Fig. 5B).

264 All genes within cluster 6 were compared to *FLC* using DTW, and the resulting distance  
265 scores were ranked from low to high (Fig. 5C). Genes in cluster 4 genes were ranked for similarity  
266 to the *VIN3* expression pattern (Fig. 5D). To validate the transcriptional profiles of the *FLC*- and  
267 *VIN3*-like genes identified from the DTW algorithm, transcripts from five genes from each

268 category were quantified in time-course samples. The results of qRT-PCR were consistent with  
269 the RNA-seq profiles (Fig. 5E, 5F). Several of the *FLC*- and *VIN3*-like genes are known floral  
270 regulators and cold-related genes that could be novel components of the vernalization pathway  
271 (Tables 4 and 5). Interestingly, of the top 10 *VIN3*-like genes, three encode factors involved in  
272 meiotic recombination (Table 5), suggesting that *VIN3* may have a role in meiotic recombination  
273 or may regulate chromatin contact.

274

### 275 ***AHL* family genes act as floral repressors in vernalization pathway**

276 In the set of 10 most *FLC*-like genes were two AT-hook family genes, *AT-HOOK MOTIF*  
277 *NUCLEAR LOCALIZE PROTEIN 21 (AHL21)* and *AT-HOOK MOTIF NUCLEAR LOCALIZE*  
278 *PROTEIN 22 (AHL22)*. qRT-PCR confirmed their expression patterns (Fig. 6B). As found in our  
279 analysis of *FLC*, stable increases of H3K27me3 were observed on both loci during and after  
280 vernalization (Fig. 6A). Previous studies have shown that *AHL* family genes are involved in control  
281 of flowering [53-56]. *AHL* family members exist in nearly all plant species sequenced so far,  
282 ranging from moss to higher plants. In *Arabidopsis*, the *AHL* family contains 29 members with  
283 conserved AT-hook motifs known to bind to AT-rich DNA sequences [57, 58]. In addition to roles  
284 in regulation of flowering *AHL* family members function in diverse aspects of plant growth and  
285 development including hypocotyl elongation, floral development, and light responses [53-56, 59,  
286 60].

287 *AHL* genes have evolved into two phylogenetic clades. Clade A are intron-less genes with  
288 only one AT-hook motif, whereas clade B are genes containing intron and one or two AT-hook  
289 motifs (Fig. S2A) [57]. Besides *AHL21* and *AHL22*, several other *AHL* family members also  
290 showed *FLC*-like transcriptional dynamics during vernalization as well as up-regulated

291 H3K27me3 marks (Fig. S2B), including *AHL19*, *AHL20*, *AHL23*, *AHL24*, *AHL25*, *AHL27*, and  
292 *AHL29*. Interestingly, all of the *FLC*-like *AHLs* belong to intron-less clade A, suggesting that clade  
293 A of *AHL* genes could be an ancient family involved in cold response.

294 To further confirm the biological function of *AHL* genes in vernalization, we obtained the  
295 knockout and overexpression lines of *AHL22* to test its flowering phenotype with or without  
296 vernalization. The *ahl22* mutants were not significantly different from wild-type plants, probably  
297 due to the highly redundant functions of *AHL* family members. However, overexpression of  
298 *AHL22* in Col-0 rendered the plant late flowering as Col-0 (*FRI*) without vernalization (Fig. 6C,  
299 top). And the flowering was accelerated after 40 days of cold treatment (Fig. 6C, bottom).  
300 Quantitative measurement indicated that the overexpression of *AHL22* resulted in elevated rosette  
301 leaves in Col-0 comparable to but less than that in *FRI*\_Col-0 without vernalization (Fig. 6C, top).  
302 Vernalization partially rescued the late-flowering phenotype in *AHL22* overexpression line but  
303 was less effective than that in *FRI*\_Col-0 (Fig. 6D), suggesting that *AHL22* might function in  
304 parallel to *FLC* in regulating downstream floral genes. Altogether, we propose that *AHL* family  
305 genes, especially genes belong to clade A, may be ancient yet novel floral regulators in  
306 vernalization pathway which were switched off by prolonged cold-induced H3K27me3 in order to  
307 assist the acceleration of flowering in *Arabidopsis thaliana*.

308

## 309 **Conclusions**

310 This work presents the first profile of dynamic transcriptome and epigenome changes  
311 during vernalization in *Arabidopsis thaliana*. RNA-seq data was collected for samples without  
312 cold exposure, with 1-hour, 1-day, 10-day, 20-day, and 40-day exposure to cold, and with a 40-  
313 day cold followed by 10 days at normal growth temperature. Analyses revealed six major clusters

314 of differentially regulated genes. Plant hormone signaling genes were among those with altered  
315 expression immediately after exposure to cold. Throughout the exposure to cold, translation-  
316 related genes were up-regulated to enabled efficient protein synthesis when enzymatic activities  
317 were limited by low temperature. Also throughout the cold exposure photosynthesis-related genes  
318 were down-regulated to prevent photo-oxidative damage caused by excessive energy production.  
319 Potential protein-binding motifs within each cluster suggest interesting candidates for further  
320 studies.

321         Genome-wide profiling of histone modifications, including H3K4me3, H3K36me3, and  
322 H3K27me3, showed a temporary reduction of H3K4me3 at photosynthesis-related genes after 40  
323 days of exposure to cold and up-regulation of H3K27me3 after 40 days of cold with and without  
324 10 days at optimal growing temperature. About one-third of the H3K27me3 peaks in all loci in the  
325 *Arabidopsis* genome that are marked with H3K27me3 were vernalization regulated; most of these  
326 genes encode transcription factors and most harbor bivalent marks of both H3K4me3 and  
327 H3K27me3. In mammalian systems, bivalent histone modifications play critical roles in  
328 embryonic development and cell lineage commitment [49-51]. Little is known about the functions  
329 of bivalent marks in *Arabidopsis*, but our finding that thousands of genes, including a large portion  
330 of transcription factors, harbor both H3K4me3 and H3K27me3 suggest that “bivalency” may allow  
331 rapid switching of transcription status of *Arabidopsis* genes critical to functions like flowering.

332         The time-course patterns of transcriptome and epigenome changes allowed us to identify  
333 novel components of the vernalization pathway. A number of *FLC*-like and *VIN3*-like genes were  
334 discovered through classification and pattern recognition. Among them, one *AHL* family gene was  
335 confirmed to be a repressor of flowering that was epigenetically silenced during vernalization.  
336 Additional candidates will be interesting targets for further studies.

337 **Declarations**

338 **Acknowledgements**

339 We wish to thank Dr. Chung-Mo Park for sharing *ahl22-2* and *ahl22-OE* seeds. The authors  
340 acknowledge the Texas Advanced Computing Center (TACC; <http://www.tacc.utexas.edu>) at The  
341 University of Texas at Austin for providing High Performance Computing resources that have  
342 contributed to the research results reported within this paper.

343

344 ***Funding***

345 This work was supported by NIH R01GM100108 and NSF IOS 1656764 to S. S.

346

347 ***Availability of data and materials***

348 The data used in this study found at GSE 130291  
349 (<https://www.ncbi.nlm.nih.gov/geo/query/acc.cgi?acc=GSE130291>).

350

351 ***Authors' contributions***

352 Y. X., S.-R. P., D.-H. K., E.-D. K., and S. S. conceived of and implemented the method, performed  
353 the experiments and data analysis. Y.X. and S.S. drafted the manuscript. SS advised on the design  
354 and implementation and interpretation of results and edited the manuscript. All authors read and  
355 approved the final manuscript.

356

357 ***Authors' current addresses:***

358 S.-R. P.: Department of Molecular & Integrative Physiology, University of Michigan, Ann  
359 Arbor, USA

360 D.-H. K.: Department of Plant Science and Technology, Chung-Ang University, Anseong, Korea

361 E.-D. K.: Department of Biology, University of Washington at Seattle, Seattle, USA

362

363 **Methods**

364 **Plant materials and growth conditions**

365 The *Arabidopsis* Col-0 with a functional *FRI* allele was used as the wild-type strain. Standard  
366 growth conditions were 22 °C with a 16-h light/8-h dark (long day) photoperiodic cycle under  
367 white fluorescent light. Seeds were surface sterilized, placed on agar medium, and grown in the  
368 dark at 4 °C for 3 days for stratification. For vernalization treatment, seedlings were grown for 7  
369 days at 22 °C, and then either harvested as NV or transferred to 4 °C under short day (8-h light/16-  
370 h dark) for 1 h (V1h), 1 day (V1d), 10 days (V10d), 20 days (V20d), and 40 days (V40d) of  
371 treatment. The T10 sample was kept at 4 °C for 40 days followed by 10 days at 22 °C before  
372 harvesting.

373

374 **RNA extraction and qRT-PCR**

375 Harvested samples were flash-frozen in liquid nitrogen. Total RNA was extracted using the  
376 Trizol/chloroform method. Extracted RNA was treated with DNase I to eliminate genomic DNA  
377 contamination. Around 2 µg of total RNA was used for cDNA synthesis using M-MLV reverse  
378 transcriptase (Promega). qRT-PCR was performed using SYBR green reaction mix (Applied  
379 Biosystems) according to the manufacturer's instructions on a Vii7 Real-Time PCR system  
380 (Applied Biosystems).

381

382 **Chromatin Immunoprecipitation (ChIP)**

383 Seedlings were crosslinked at 4 °C with 1% formaldehyde solution under vacuum for 25 min. The  
384 reaction was terminated by addition of 0.125 M glycine. Crosslinked seedlings were rinsed in  
385 distilled water and then flash frozen in liquid nitrogen. ChIP was performed following the Abcam

386 ChIP protocol (<https://www.abcam.com/protocols/chip-using-plant-samples---arabidopsis>) with  
387 minor adjustments. Aliquots of eluted DNA were used for qRT-PCR and for sequencing.

388

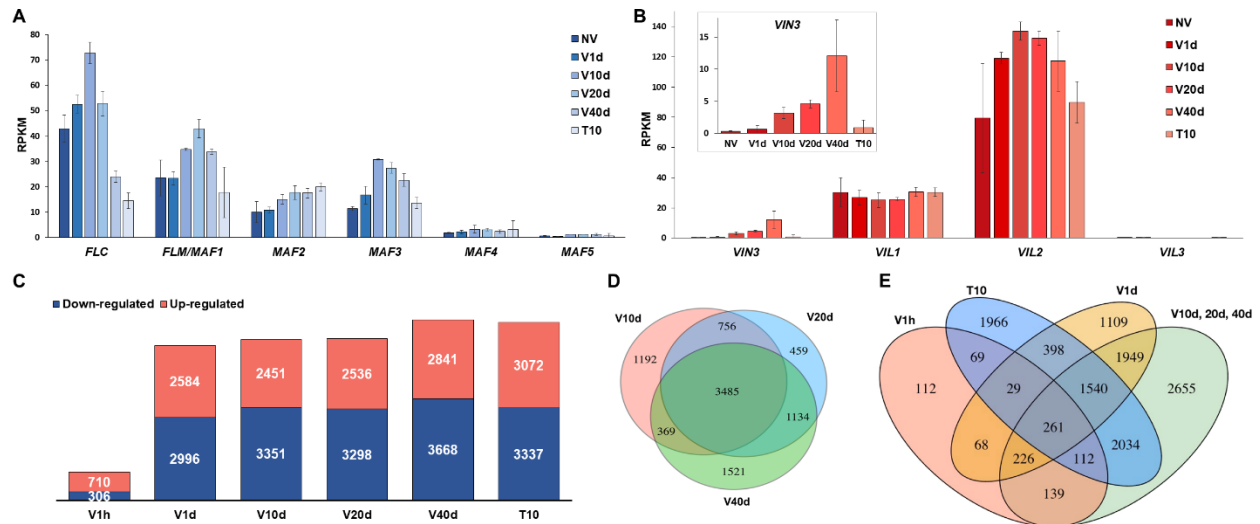
### 389 **Library construction and sequencing**

390 Ribosomal RNAs were depleted from the extracted RNA using RiboMinus Plant Kit (Thermo  
391 Fisher). The polyA-enrichment procedure was omitted in order to capture the total RNA. Library  
392 construction was done using NEBNext Ultra Directional RNA Library Prep Kit for Illumina (NEB)  
393 following the manufacturer's instructions. Libraries were sequenced on an Illumina HiSeq2500  
394 platform by the Genomic Sequencing and Analysis Facility at the University of Texas at Austin.

395

### 396 **Sequence alignment and analysis**

397 The raw reads were trimmed and quality-filtered before aligned to the *Arabidopsis thaliana*  
398 TAIR10 transcriptome by Tophat (RNA-seq) or Bowtie2 (ChIP-seq). Aligned reads were  
399 converted to digital counts using Rsubread and were analyzed using edgeR. Differentially  
400 expressed genes were identified based on a 0.05 p-value and two-fold difference cut-off. Motif  
401 analysis was done by using MEME. Peaks were called by MACS2. GO analysis was done using  
402 DAVID. Clustering was done in Python using sikit-learn packages.



403

404

405 **Figure 1. Changes in the *Arabidopsis* transcriptome during the course of vernalization.**

406 (A) Quantitative measurement of expression levels of *FLC* family genes over a time course during

407 vernalization as in Reads Per Kilobase of transcript, per Million mapped reads (RPKM). Error bars

408 were generated based on normalized read counts within each locus from 2 biological replicates.

409 (B) Quantitative measurement of expression levels of *VIN3* family genes over a time course during

410 vernalization as in RPKM. Error bars were generated based on normalized read counts within each

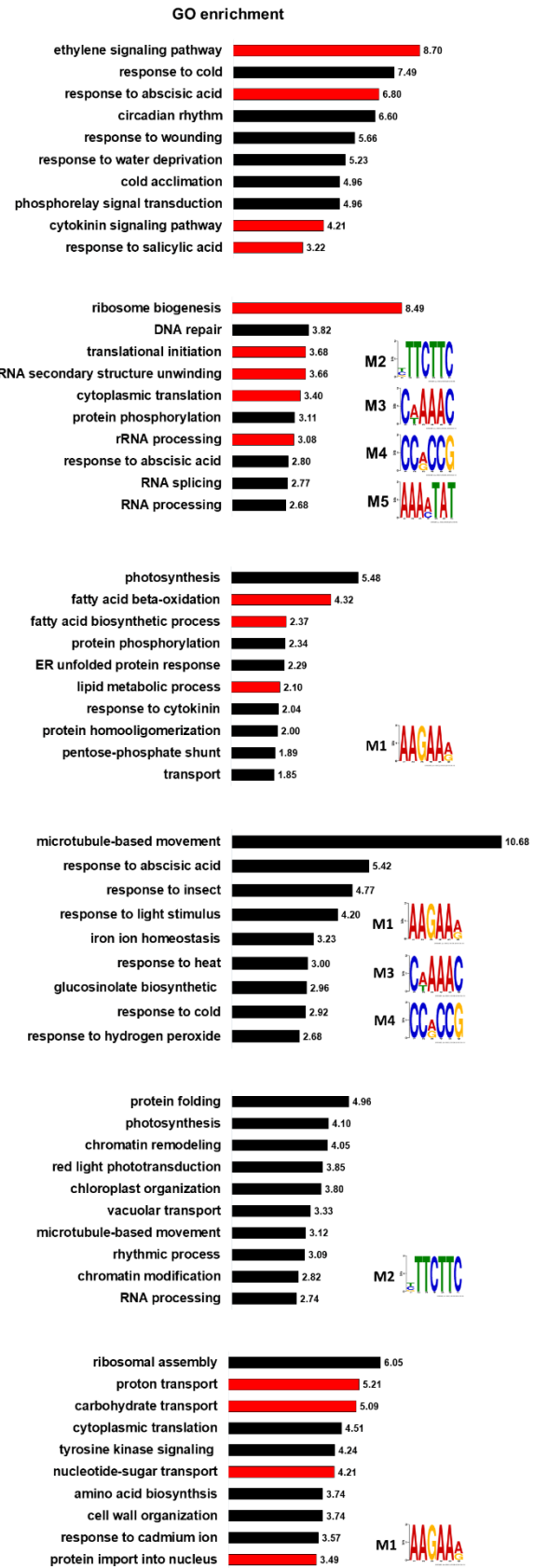
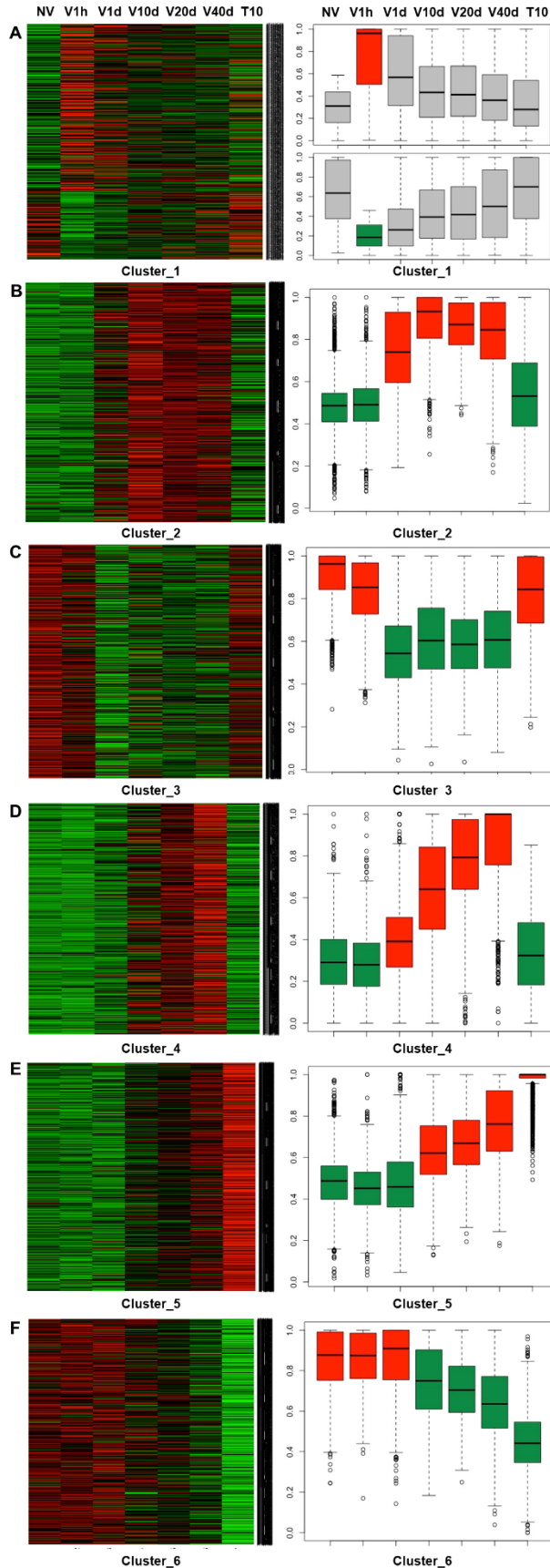
411 locus from 2 biological replicates. (C) Bar graph showing total numbers of differentially up-

412 regulated (red) and down-regulated (blue) genes at each time point relative to NV. (D) Venn

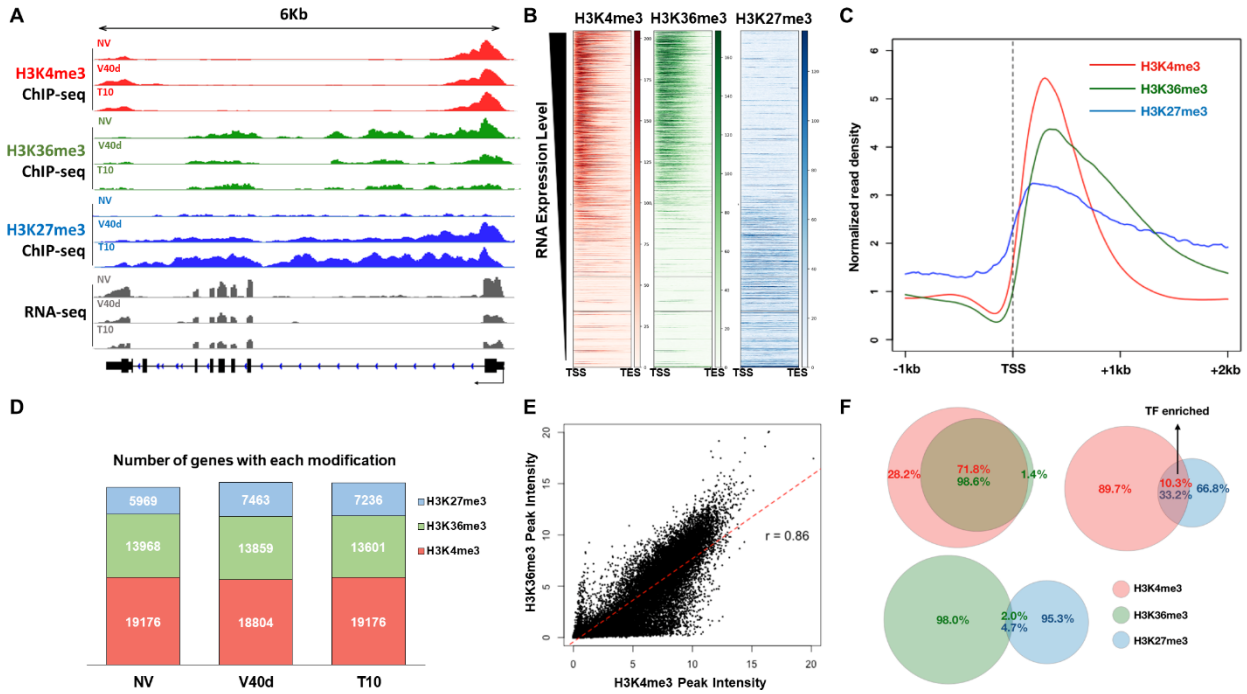
413 diagram showing the overlapping and uniquely differentially regulated genes at V10d, V20d, and

414 V40d. (E) Venn diagram showing the overlapping and uniquely differentially regulated genes at

415 V1h, V1d, V10d/20d/40d, and T10.



417 **Figure 2. Clustering analysis of transcriptome data collected during vernalization.**  
418 (A-F) Clusters 1 to 6, respectively, were generated from k-means clustering of transcription  
419 profiles obtained over the time course of vernalization. Shown from left to right for genes in the  
420 indicated cluster are heatmaps of gene expression at each time point, normalized box plots of genes  
421 expression at each time point, enriched GO terms, and motifs enriched within clustered genes if  
422 detected.  
423



425

426

427 **Figure 3. Genome-wide analysis of histone modifications during the course of vernalization.**

428 (A) Genome browser illustration of normalized ChIP-seq and RNA-seq results at *FLC* locus.

429 H3K4me3 tracks are shown in red, H3K36me3 in green, and H3K27me3 in blue. RNA-seq results

430 are shown in grey colors. (B) Heatmaps of H3K4me3 (red), H3K36me3 (green), and H3K27me3

431 (blue) over all coding genes in *Arabidopsis* genome. Each row represents the normalized read

432 density from transcription start site (TSS) to transcription end site (TES) of each gene, ranked by

433 transcription level from the highest (top) to the lowest (bottom). (C) Averaged profiles of

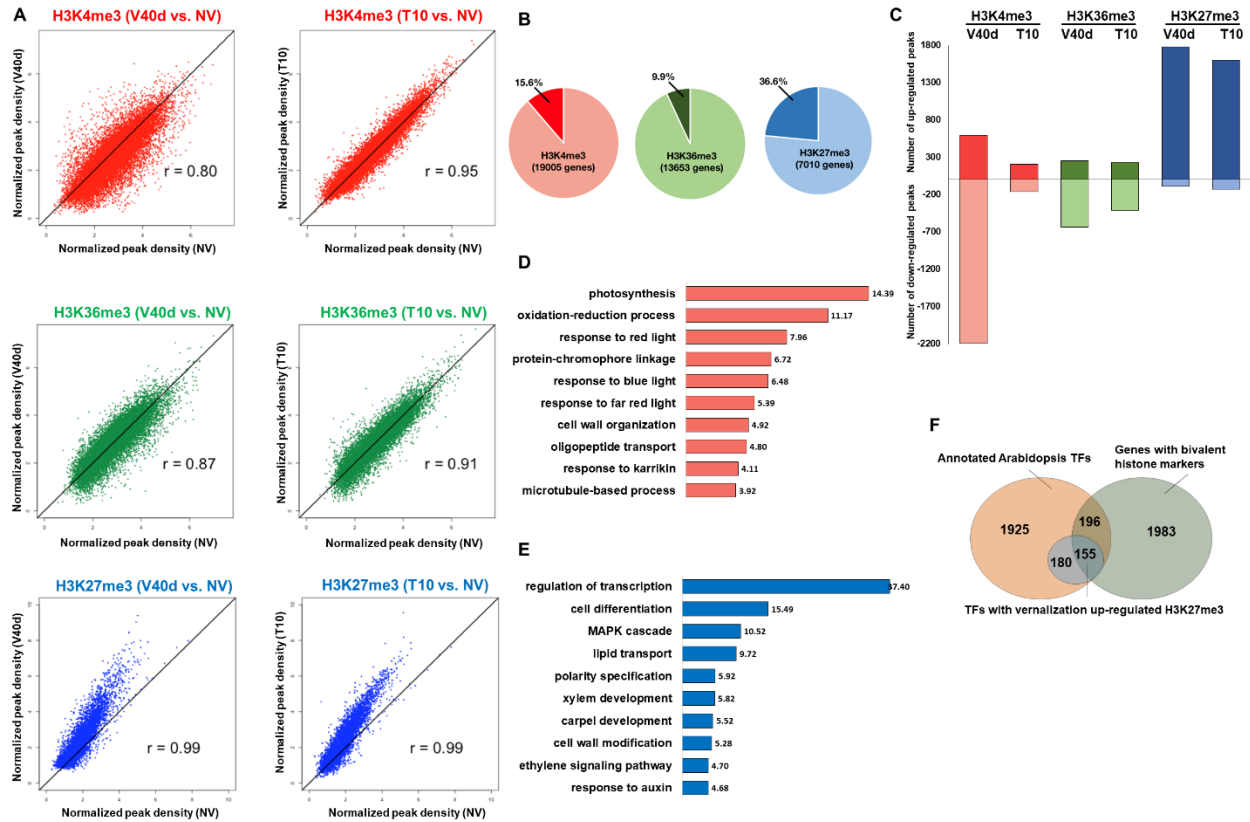
434 H3K4me3 (red), H3K36me3 (green), and H3K27me3 (blue) distributions around TSS regions over

435 all coding genes in *Arabidopsis* genome. (D) Bar graph showing total number of peaks called by

436 MACS2 within each sample. (E) Correlation plot of genome-wide H3K4me3 and H3K36me3

437 densities. (F) Venn diagrams showing overlapped among different histone marks.

438



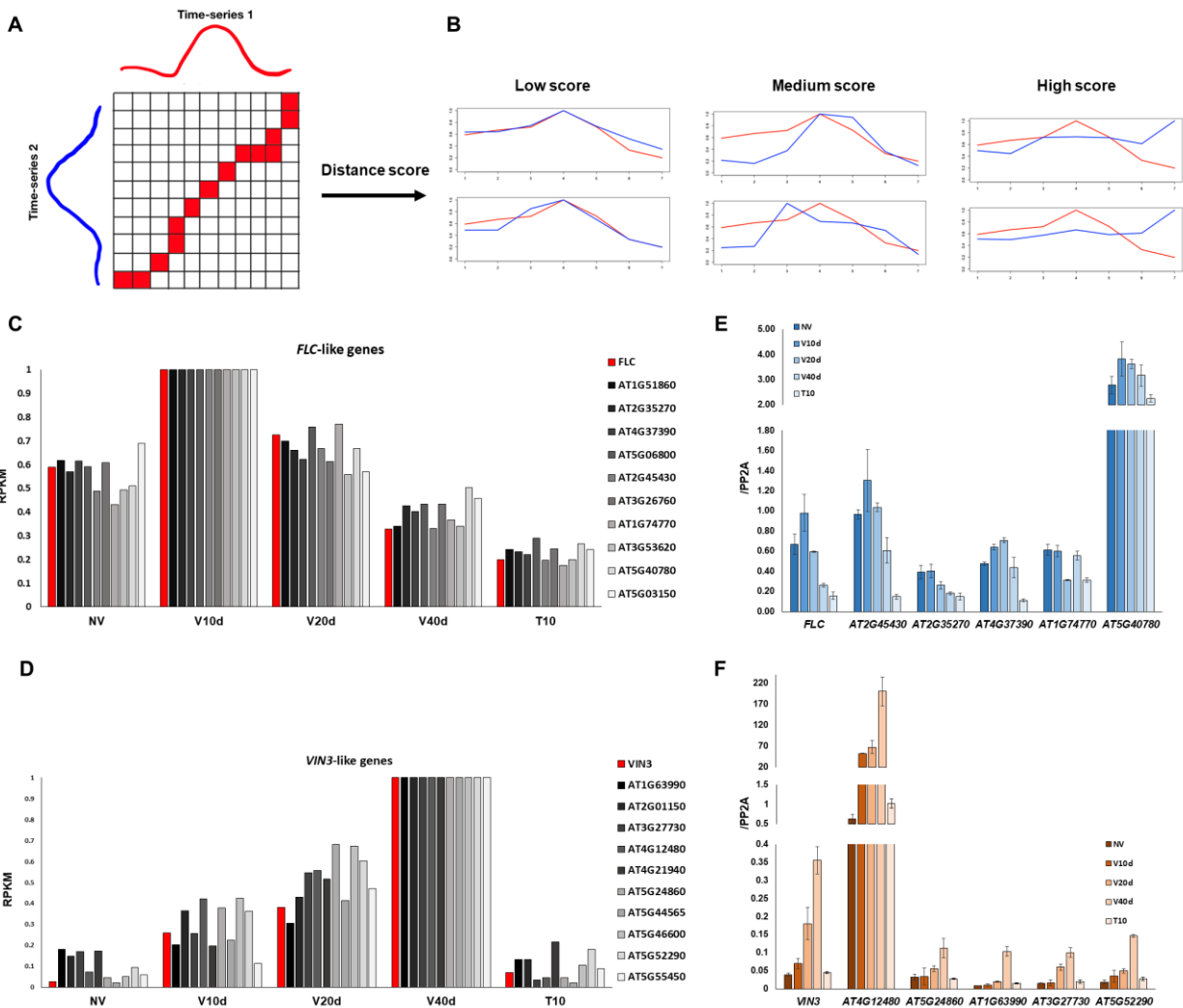
439

440

441 **Figure 4. Characteristics of histone modification-enriched loci during the course of**  
442 **vernalization.**

443 (A) Correlation plots of densities of H3K4me3 in red, H3K36me3 in green, and H3K27me3 in  
444 blue in V40d vs. NV (left) and T10 vs. NV (right) samples. (B) Pie graph showing the percentages  
445 of histone modification peaks differentially regulated during vernalization. (C) Bar graph showing  
446 the number of vernalization up-regulated (darker hues) and down-regulated (lighter hues)  
447 H3K4me3 (red), H3K36me3 (green), and H3K27me3 (blue) peaks. (D) Bar graph showing top  
448 GO terms ranked by enrichment score from H3K4me3 temporarily down-regulated loci with *p*-  
449 value. (E) Bar graph showing top GO terms ranked by enrichment score from H3K27me3 up-  
450 regulated loci with *p*-value.

451



452

453

454 **Figure 5. Identification of genes with expression similar to that of *FLC* and *VIN3* using the**  
 455 **dynamic warping algorithm.**

456 (A) Illustration of Dynamic Time Warping algorithm. (B) Examples of sequences with low (left),

457 medium (middle), and high (right) distance scores. (C) Bar graph showing the RNA-seq results

458 of the 10 genes (in shades of grey) that most closely resemble the vernalization-mediated

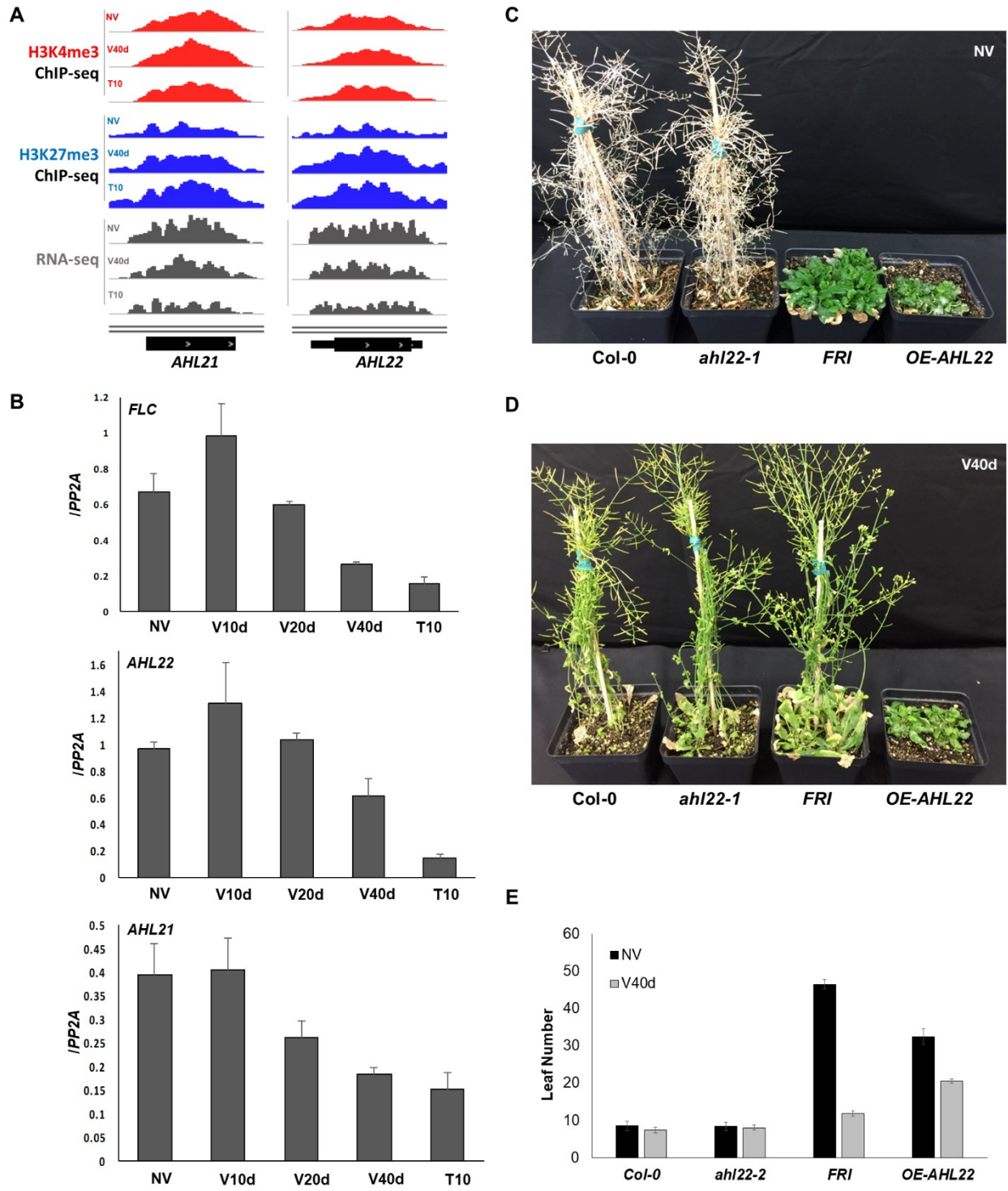
459 repression pattern of *FLC* (red). (D) Bar graph showing the RNA-seq results of the 10 genes (in

460 shades of grey) that most closely resemble the vernalization-mediated induction pattern of *VIN3*

461 (red). (E) qRT-PCR validation of expression patterns of *FLC*-like genes over time. Expression

462 levels are relative to *PP2A*. ( $n = 3$ ) (F) qRT-PCR validation of *VIN3*-like genes. Expression levels  
463 are relative to *PP2A* ( $n = 3$ ).

464



465

466

467 **Figure 6. Phenotypes of *AHL22* knockout and overexpression strains.**

468 (A) Genome browser tracks showing H3K4me3 (red), H3K27me3 (blue), and RNA-seq (grey)  
469 results at *AHL21* and *AHL22* loci during vernalization. (B) Validation of *FLC*, *AHL21*, and *AHL22*  
470 expression levels using q-RT-PCR. ( $n = 3$ ) (C) Flowering phenotypes of Col-0, *AHL22*-null mutant,  
471 *FRI*-null mutant, and *AHL22* overexpression lines with (bottom) or without (top) vernalization. (D)  
472 Quantification of flowering time based on counting rosette leaf numbers ( $n = 12$ ).  
473

474 Table 1. Motifs enriched in each cluster of genes differentially regulated during  
 475 vernalization.

476

	Motif 1	Motif 2	Motif 3	Motif 4	Motif 5
Cluster_2					
Cluster_3					
Cluster_4					
Cluster_5					
Cluster_6					

477  
 478

479 **Table 2. Transcription factors (TFs) with binding motifs similar to those identified in genes**  
 480 **differentially regulated during vernalization.**  
 481

	<b>Motif 1 (M1)</b>	<b>Motif 2 (M2)</b>	<b>Motif 3 (M3)</b>	<b>Motif 4 (M4)</b>	<b>Motif 5 (M5)</b>
<b>Matched TFs</b>	NTL4, NAC2	NTL8	CRC	ERF17, ERF38, ERF74, WIND3, WIND4	RVE1, RVE4, RVE5, RVE8, LHY, EPR1
<b>Family</b>	NAC domain family	NAC domain family	Plant-specific YABBY family	DREB subfamily of ERF/AP2 family	Homeodomain-like family
<b>Reported functions</b>	drought response, JA biosynthesis, salt stress, embryogenesis, stamen development	salt stress, flowering, trichome formation	fatty acid biosynthesis, carpel development	hypoxia response, osmotic stress, ethylene signaling, redox sensing	circadian clock, photoperiodic flowering, auxin signaling, chlorophyll synthesis

482  
 483

484 **Table 3. Functional annotations of transcription factors with vernalization-induced**  
 485 **H3K27me3 up-regulation.**  
 486

Functional annotation	Number of genes	Enrichment score	<i>P</i> -value
cell differentiation	59	40.82	1.30E-13
ethylene signaling pathway	30	17.4	1.00E-19
flower development	25	11.12	2.20E-13
carpel development	10	9.4	1.30E-11
ovule development	11	6.85	5.40E-09
regulation of secondary cell wall biogenesis	8	6.82	5.20E-09
vegetative to reproductive phase transition of meristem	14	6.1	3.30E-08
gibberellic acid signaling pathway	11	4.82	6.50E-07
specification of flora organ identity	6	4.57	1.30E-06
trichome differentiation	7	4.32	2.40E-06
transmitting tissue development	4	3.42	2.20E-05
auxin signaling pathway	14	3.21	3.80E-05

487  
 488

489 **Table 4. Genes with expression patterns similar to *FLC* during the course of vernalization.**  
 490

<b>Locus</b>	<b>Name</b>	<b>Protein domain</b>	<b>Reported function</b>
AT1G51860	-	LRR, protein kinase	-
AT2G45430	AHL22	AT-hook DNA-binding	regulation of flowering
AT2G35270	AHL21	AT-hook DNA-binding	patterning and differentiation of reproductive organs
AT4G37390	AUR3	GH3 auxin-responsive	negative component in auxin signaling
AT5G06800	-	Myb-like DNA-binding	-
AT3G26760	-	glucose dehydrogenase	-
AT1G74770	BTSL1	zinc finger	negative regulator of iron deficiency
AT3G53620	PPA4	pyrophosphatase	regulate pyrophosphate levels
AT5G40780	LHT1	transmembrane	high-affinity transporter for cellular amino acid uptake
AT5G03150	JKD	zinc finger	epidermal patterning in root meristem

491  
 492

493 **Table 5. Genes with expression patterns similar to *VIN3* during the course of vernalization.**  
 494  
 495

<b>Locus</b>	<b>Name</b>	<b>Protein domain</b>	<b>Reported function</b>
AT5G44565	-	transmembrane	-
AT5G55450	LTP4.4	-	lipid transport and pathogen resistance
AT2G01150	RHA2B	zinc finger	ABA signaling and drought response
AT1G63990	SPO11-2	DNA topoisomerase VI	regulate meiotic recombination
AT3G27730	MER3	DEAD-like helicase	required for meiotic crossover formation
AT4G12480	EARLI1	plant lipid transfer	resistance to low temperature and fungal infection
AT4G21940	CPK15	protein kinase	-
AT5G52290	SHOC1	similar to XPF endonucleases	required for class-I meiotic crossover formation
AT5G24860	FPF1	-	regulate the competence to flowering
AT5G46600	-	malate transporter	-

496  
 497  
 498

499 **References**

- 500 1. Werner JD, Borevitz JO, Uhlenhaut NH, Ecker JR, Chory J, Weigel D: **FRIGIDA-independent**  
501 **variation in flowering time of natural Arabidopsis thaliana accessions.** *Genetics* 2005,  
502 **170:1197-1207.**
- 503 2. Shindo C, Aranzana MJ, Lister C, Baxter C, Nicholls C, Nordborg M, Dean C: **Role of**  
504 **FRIGIDA and FLOWERING LOCUS C in determining variation in flowering time of**  
505 **Arabidopsis.** *Plant Physiol* 2005, **138:1163-1173.**
- 506 3. Coustham V, Li P, Strange A, Lister C, Song J, Dean C: **Quantitative modulation of**  
507 **polycomb silencing underlies natural variation in vernalization.** *Science* 2012, **337:584-**  
508 **587.**
- 509 4. Michaels SD, Amasino RM: **FLOWERING LOCUS C encodes a novel MADS domain protein**  
510 **that acts as a repressor of flowering.** *Plant Cell* 1999, **11:949-956.**
- 511 5. Lee J, Lee I: **Regulation and function of SOC1, a flowering pathway integrator.** *J Exp Bot*  
512 2010, **61:2247-2254.**
- 513 6. Hepworth SR, Valverde F, Ravenscroft D, Mouradov A, Coupland G: **Antagonistic**  
514 **regulation of flowering-time gene SOC1 by CONSTANS and FLC via separate promoter**  
515 **motifs.** *Embo J* 2002, **21:4327-4337.**
- 516 7. Johanson U, West J, Lister C, Michaels S, Amasino R, Dean C: **Molecular analysis of**  
517 **FRIGIDA, a major determinant of natural variation in Arabidopsis flowering time.**  
518 *Science* 2000, **290:344-347.**
- 519 8. Schmitz RJ, Hong L, Michaels S, Amasino RM: **FRIGIDA-ESSENTIAL 1 interacts genetically**  
520 **with FRIGIDA and FRIGIDA-LIKE 1 to promote the winter-annual habit of Arabidopsis**  
521 **thaliana.** *Development* 2005, **132:5471-5478.**
- 522 9. Choi K, Kim S, Kim SY, Kim M, Hyun Y, Lee H, Choe S, Kim SG, Michaels S, Lee I:  
523 **SUPPRESSOR OF FRIGIDA3 encodes a nuclear ACTIN-RELATED PROTEIN6 required for**  
524 **floral repression in Arabidopsis.** *Plant Cell* 2005, **17:2647-2660.**
- 525 10. Kim S, Choi K, Park C, Hwang HJ, Lee I: **SUPPRESSOR OF FRIGIDA4, encoding a C2H2-Type**  
526 **zinc finger protein, represses flowering by transcriptional activation of Arabidopsis**  
527 **FLOWERING LOCUS C.** *Plant Cell* 2006, **18:2985-2998.**
- 528 11. Geraldo N, Baurle I, Kidou S, Hu X, Dean C: **FRIGIDA delays flowering in Arabidopsis via a**  
529 **cotranscriptional mechanism involving direct interaction with the nuclear cap-binding**  
530 **complex.** *Plant Physiol* 2009, **150:1611-1618.**
- 531 12. Jiang D, Gu X, He Y: **Establishment of the winter-annual growth habit via FRIGIDA-**  
532 **mediated histone methylation at FLOWERING LOCUS C in Arabidopsis.** *Plant Cell* 2009,  
533 **21:1733-1746.**
- 534 13. Hu X, Kong X, Wang C, Ma L, Zhao J, Wei J, Zhang X, Loake GJ, Zhang T, Huang J, Yang Y:  
535 **Proteasome-mediated degradation of FRIGIDA modulates flowering time in Arabidopsis**  
536 **during vernalization.** *Plant Cell* 2014, **26:4763-4781.**
- 537 14. Li Z, Jiang D, He Y: **FRIGIDA establishes a local chromosomal environment for**  
538 **FLOWERING LOCUS C mRNA production.** *Nat Plants* 2018, **4:836-846.**
- 539 15. Sheldon CC, Rouse DT, Finnegan EJ, Peacock WJ, Dennis ES: **The molecular basis of**  
540 **vernalization: the central role of FLOWERING LOCUS C (FLC).** *Proc Natl Acad Sci U S A*  
541 2000, **97:3753-3758.**

- 542 16. Moon J, Suh SS, Lee H, Choi KR, Hong CB, Paek NC, Kim SG, Lee I: **The SOC1 MADS-box**  
543 **gene integrates vernalization and gibberellin signals for flowering in Arabidopsis.** *Plant*  
544 *J* 2003, **35**:613-623.
- 545 17. Michaels SD, Himelblau E, Kim SY, Schomburg FM, Amasino RM: **Integration of flowering**  
546 **signals in winter-annual Arabidopsis.** *Plant Physiol* 2005, **137**:149-156.
- 547 18. Searle I, He Y, Turck F, Vincent C, Fornara F, Krober S, Amasino RA, Coupland G: **The**  
548 **transcription factor FLC confers a flowering response to vernalization by repressing**  
549 **meristem competence and systemic signaling in Arabidopsis.** *Genes Dev* 2006, **20**:898-  
550 912.
- 551 19. Helliwell CA, Wood CC, Robertson M, James Peacock W, Dennis ES: **The Arabidopsis FLC**  
552 **protein interacts directly in vivo with SOC1 and FT chromatin and is part of a high-**  
553 **molecular-weight protein complex.** *Plant J* 2006, **46**:183-192.
- 554 20. Gu X, Le C, Wang Y, Li Z, Jiang D, He Y: **Arabidopsis FLC clade members form flowering-**  
555 **repressor complexes coordinating responses to endogenous and environmental cues.**  
556 *Nat Commun* 2013, **4**:1947.
- 557 21. Chen M, Penfield S: **Feedback regulation of COOLAIR expression controls seed dormancy**  
558 **and flowering time.** *Science* 2018, **360**:1014-1017.
- 559 22. Luo X, Chen T, Zeng X, He D, He Y: **Feedback Regulation of FLC by FLOWERING LOCUS T**  
560 **(FT) and FD through a 5' FLC Promoter Region in Arabidopsis.** *Mol Plant* 2019, **12**:285-  
561 288.
- 562 23. Sheldon CC, Hills MJ, Lister C, Dean C, Dennis ES, Peacock WJ: **Resetting of FLOWERING**  
563 **LOCUS C expression after epigenetic repression by vernalization.** *Proc Natl Acad Sci U S*  
564 *A* 2008, **105**:2214-2219.
- 565 24. Sung S, Amasino RM: **Vernalization in Arabidopsis thaliana is mediated by the PHD finger**  
566 **protein VIN3.** *Nature* 2004, **427**:159-164.
- 567 25. Sung S, He Y, Eshoo TW, Tamada Y, Johnson L, Nakahigashi K, Goto K, Jacobsen SE,  
568 Amasino RM: **Epigenetic maintenance of the vernalized state in Arabidopsis thaliana**  
569 **requires LIKE HETEROCHROMATIN PROTEIN 1.** *Nat Genet* 2006, **38**:706-710.
- 570 26. Sung S, Amasino RM: **Molecular genetic studies of the memory of winter.** *J Exp Bot* 2006,  
571 **57**:3369-3377.
- 572 27. Mylne JS, Barrett L, Tessadori F, Mesnage S, Johnson L, Bernatavichute YV, Jacobsen SE,  
573 Fransz P, Dean C: **LHP1, the Arabidopsis homologue of HETEROCHROMATIN PROTEIN1,**  
574 **is required for epigenetic silencing of FLC.** *Proc Natl Acad Sci U S A* 2006, **103**:5012-5017.
- 575 28. De Lucia F, Crevillen P, Jones AM, Greb T, Dean C: **A PHD-polycomb repressive complex**  
576 **2 triggers the epigenetic silencing of FLC during vernalization.** *Proc Natl Acad Sci U S A*  
577 2008, **105**:16831-16836.
- 578 29. Kim DH, Zografos BR, Sung S: **Mechanisms underlying vernalization-mediated VIN3**  
579 **induction in Arabidopsis.** *Plant Signal Behav* 2010, **5**.
- 580 30. Heo JB, Sung S: **Vernalization-mediated epigenetic silencing by a long intronic noncoding**  
581 **RNA.** *Science* 2011, **331**:76-79.
- 582 31. Rosa S, De Lucia F, Mylne JS, Zhu D, Ohmido N, Pendle A, Kato N, Shaw P, Dean C: **Physical**  
583 **clustering of FLC alleles during Polycomb-mediated epigenetic silencing in vernalization.**  
584 *Genes Dev* 2013, **27**:1845-1850.

- 585 32. Crevillen P, Sonmez C, Wu Z, Dean C: **A gene loop containing the floral repressor FLC is**  
586 **disrupted in the early phase of vernalization.** *EMBO J* 2013, **32**:140-148.
- 587 33. Questa JI, Song J, Geraldo N, An H, Dean C: **Arabidopsis transcriptional repressor VAL1**  
588 **triggers Polycomb silencing at FLC during vernalization.** *Science* 2016, **353**:485-488.
- 589 34. Kim DH, Sung S: **Vernalization-Triggered Intragenic Chromatin Loop Formation by Long**  
590 **Noncoding RNAs.** *Dev Cell* 2017, **40**:302-312 e304.
- 591 35. Kim SY, He Y, Jacob Y, Noh YS, Michaels S, Amasino R: **Establishment of the vernalization-**  
592 **responsive, winter-annual habit in Arabidopsis requires a putative histone H3 methyl**  
593 **transferase.** *Plant Cell* 2005, **17**:3301-3310.
- 594 36. Tamada Y, Yun JY, Woo SC, Amasino RM: **ARABIDOPSIS TRITHORAX-RELATED7 is**  
595 **required for methylation of lysine 4 of histone H3 and for transcriptional activation of**  
596 **FLOWERING LOCUS C.** *Plant Cell* 2009, **21**:3257-3269.
- 597 37. Whittaker C, Dean C: **The FLC Locus: A Platform for Discoveries in Epigenetics and**  
598 **Adaptation.** *Annu Rev Cell Dev Biol* 2017, **33**:555-575.
- 599 38. Csorba T, Questa JI, Sun Q, Dean C: **Antisense COOLAIR mediates the coordinated**  
600 **switching of chromatin states at FLC during vernalization.** *Proc Natl Acad Sci U S A* 2014,  
601 **111**:16160-16165.
- 602 39. Swiezewski S, Liu F, Magusin A, Dean C: **Cold-induced silencing by long antisense**  
603 **transcripts of an Arabidopsis Polycomb target.** *Nature* 2009, **462**:799-802.
- 604 40. Yuan W, Luo X, Li Z, Yang W, Wang Y, Liu R, Du J, He Y: **A cis cold memory element and a**  
605 **trans epigenome reader mediate Polycomb silencing of FLC by vernalization in**  
606 **Arabidopsis.** *Nat Genet* 2016, **48**:1527-1534.
- 607 41. Sun M, Qi X, Hou L, Xu X, Zhu Z, Li M: **Gene Expression Analysis of Pak Choi in Response**  
608 **to Vernalization.** *PLoS One* 2015, **10**:e0141446.
- 609 42. Liu C, Wang C, Wang G, Becker C, Zaidem M, Weigel D: **Genome-wide analysis of**  
610 **chromatin packing in Arabidopsis thaliana at single-gene resolution.** *Genome Res* 2016,  
611 **26**:1057-1068.
- 612 43. Oquist G, Huner NP: **Photosynthesis of overwintering evergreen plants.** *Annu Rev Plant*  
613 *Biol* 2003, **54**:329-355.
- 614 44. Yang CY, Hsu FC, Li JP, Wang NN, Shih MC: **The AP2/ERF transcription factor**  
615 **AtERF73/HRE1 modulates ethylene responses during hypoxia in Arabidopsis.** *Plant*  
616 *Physiol* 2011, **156**:202-212.
- 617 45. Gasch P, Fundinger M, Muller JT, Lee T, Bailey-Serres J, Mustroph A: **Redundant ERF-VII**  
618 **Transcription Factors Bind to an Evolutionarily Conserved cis-Motif to Regulate**  
619 **Hypoxia-Responsive Gene Expression in Arabidopsis.** *Plant Cell* 2016, **28**:160-180.
- 620 46. Bond DM, Wilson IW, Dennis ES, Pogson BJ, Jean Finnegan E: **VERNALIZATION**  
621 **INSENSITIVE 3 (VIN3) is required for the response of Arabidopsis thaliana seedlings**  
622 **exposed to low oxygen conditions.** *Plant J* 2009.
- 623 47. Gibbs DJ, Tedds HM, Labandera AM, Bailey M, White MD, Hartman S, Sprigg C, Mogg SL,  
624 Osborne R, Dambire C, et al: **Oxygen-dependent proteolysis regulates the stability of**  
625 **angiosperm polycomb repressive complex 2 subunit VERNALIZATION 2.** *Nat Commun*  
626 2018, **9**:5438.
- 627 48. Vastenhouw NL, Schier AF: **Bivalent histone modifications in early embryogenesis.** *Curr*  
628 *Opin Cell Biol* 2012, **24**:374-386.

- 629 49. Zaidi SK, Fietze SE, Gordon JA, Heath JL, Messier T, Hong D, Boyd JR, Kang M, Imbalzano  
630 AN, Lian JB, et al: **Bivalent Epigenetic Control of Oncofetal Gene Expression in Cancer.**  
631 *Mol Cell Biol* 2017, **37**.
- 632 50. Harikumar A, Meshorer E: **Chromatin remodeling and bivalent histone modifications in**  
633 **embryonic stem cells.** *EMBO Rep* 2015, **16**:1609-1619.
- 634 51. Voigt P, Tee WW, Reinberg D: **A double take on bivalent promoters.** *Genes Dev* 2013,  
635 **27**:1318-1338.
- 636 52. Sakoe H, Chiba S: **Dynamic-Programming Algorithm Optimization for Spoken Word**  
637 **Recognition.** *Ieee Transactions on Acoustics Speech and Signal Processing* 1978, **26**:43-  
638 49.
- 639 53. Xu Y, Gan ES, He Y, Ito T: **Flowering and genome integrity control by a nuclear matrix**  
640 **protein in Arabidopsis.** *Nucleus* 2013, **4**:274-276.
- 641 54. Ng KH, Yu H, Ito T: **AGAMOUS controls GIANT KILLER, a multifunctional chromatin**  
642 **modifier in reproductive organ patterning and differentiation.** *PLoS Biol* 2009,  
643 **7**:e1000251.
- 644 55. Yun J, Kim YS, Jung JH, Seo PJ, Park CM: **The AT-hook motif-containing protein AHL22**  
645 **regulates flowering initiation by modifying FLOWERING LOCUS T chromatin in**  
646 **Arabidopsis.** *J Biol Chem* 2012, **287**:15307-15316.
- 647 56. Xiao C, Chen F, Yu X, Lin C, Fu YF: **Over-expression of an AT-hook gene, AHL22, delays**  
648 **flowering and inhibits the elongation of the hypocotyl in Arabidopsis thaliana.** *Plant Mol*  
649 *Biol* 2009, **71**:39-50.
- 650 57. Zhao J, Favero DS, Peng H, Neff MM: **Arabidopsis thaliana AHL family modulates**  
651 **hypocotyl growth redundantly by interacting with each other via the PPC/DUF296**  
652 **domain.** *Proc Natl Acad Sci U S A* 2013, **110**:E4688-4697.
- 653 58. Zhao J, Favero DS, Qiu J, Roalson EH, Neff MM: **Insights into the evolution and**  
654 **diversification of the AT-hook Motif Nuclear Localized gene family in land plants.** *BMC*  
655 *Plant Biol* 2014, **14**:266.
- 656 59. Street IH, Shah PK, Smith AM, Avery N, Neff MM: **The AT-hook-containing proteins**  
657 **SOB3/AHL29 and ESC/AHL27 are negative modulators of hypocotyl growth in**  
658 **Arabidopsis.** *Plant J* 2008, **54**:1-14.
- 659 60. Lim PO, Kim Y, Breeze E, Koo JC, Woo HR, Ryu JS, Park DH, Beynon J, Tabrett A, Buchanan-  
660 Wollaston V, Nam HG: **Overexpression of a chromatin architecture-controlling AT-hook**  
661 **protein extends leaf longevity and increases the post-harvest storage life of plants.**  
662 *Plant J* 2007, **52**:1140-1153.  
663